Global Journal of Engineering and Technology Advances
eISSN: 2582-5003
Cross Ref DOI: 10.30574/gjeta
Journal homepage: https://gjeta.com/

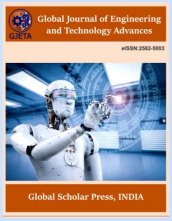

(RESEARCH ARTICLE)

Check for updates

How to avoid the impact of TCSC on protection schemes

Enrique Reyes-Archundia *, Marco V. Chávez-Báez, Arturo Méndez-Patiño, José A. Gutiérrez-Gnecchi, Juan C. Olivares-Rojas and María C. García-Ramírez

Division of Graduate Studies and Research, National Technological of Mexico / Technological Institute of Morelia, Morelia, Mexico.

Global Journal of Engineering and Technology Advances, 2022, 13(03), 053–065

Publication history: Received on 29 October 2022; revised on 12 December 2022; accepted on 15 December 2022

Article DOI: https://doi.org/10.30574/gjeta.2022.13.3.0200

Abstract

Because of its undoubted advantages, the Thyristor Controlled Series Capacitor (TCSC) is one of the most widely used power-electronic controllers in power systems. However, the TCSC has also been a cause of concern in protective relaying because of its impact on the impedance seen by conventional distance relays, which may lead to an incorrect assessment of fault distance and, consequently, an erroneous relay tripping. To overcome these difficulties, this paper proposes using schemes based on traveling waves for protecting TCSC series compensated transmission lines. Since the method avoids using impedance-based techniques, it is not prone to under-reach or over-reach problems, among others. The approach is based on traveling wave analysis using the discrete wavelet transform. The different case studies show the effectiveness and accuracy of the proposed algorithm in a TCSC environment.

Keywords: Thyristor-controlled series capacitor; Wavelet transform; Protection algorithm; Traveling wave

1. Introduction

In the last decade, power electronic devices have been increasingly introduced into electrical power systems. This trend will soon continue in the Smart Grid concept framework.

Power electronic controllers for Flexible AC Transmission Systems (FACTS) have undoubted advantages for improving power system operational characteristics. One of the most widely used FACTS devices is the Thyristor Controlled Series Capacitor (TCSC) which can perform several functions. For instance, improving voltage regulation (1), enhancing transmission line capability (2), (3), improving power system stability (4), and mitigating power system oscillations and perturbations (5).

However, sometimes the interaction between FACTS controllers and other power system components may be a source of concern for other electrical engineering areas. For instance, when protecting long transmission lines-compensated with TCSC controllers. In this scheme, it is well known that under fault conditions, the distance to the fault is not accurately calculated by conventional distance relays (6).

This inaccurate assessment of the fault distance is explained by the interaction between the transmission line and the TCSC, which sometimes leads to sudden changes in the impedance calculated by distance relays, depending on the line compensation level and fault location. Conventional line protection algorithms used in distance relays are not prepared for dealing with these scenarios, and therefore erroneous relay tripping in the presence of TCSC devices may occur (7).

* Corresponding author: E. Reyes-Archundia
Division of Graduate Studies and Research, National Technological of Mexico / Technological Institute of Morelia, Morelia, Mexico.

Several algorithms and techniques have been proposed in the literature to improve fault detection, and location in TCSC series compensated transmission lines. In 2004, an approach suggested using higher components in the frequency spectrum generated by the TCSC to detect whether the fault is located before or after the TCSC (8). In 2007, a Vector Machine Support (VMS) technique was proposed to improve fault detection and location (9). In 2011, Ahsaee et al. proposed an optimization method and the use of measurements in both lines ends to calculate the distance to the fault considering the propagation speed of electromagnetic waves (10). In 2014, Nobakhti used the time domain modeling of a transmission line to fault location (11). It should be mentioned that the above techniques are based on current or impedance measurements, and they use at least half of the cycle window. Recently, some approaches have considered renewable sources integration, as Wind Farms (12,13).

Traveling wave techniques have been extensively used to detect and locate faults in AC (14)(15)(16) and HVDC transmission lines (17,18), (19). They are faster to detect and discriminate faults than conventional impedance-based schemes (20). However, its application in a FACTS environment has been limited. There is concern about the impact that higher harmonic frequencies generated by the TCSC might have on the overall accuracy and reliability of a traveling waves-based scheme. In particular, it is feared that TCSC-generated harmonics may distort the high-frequency pattern of reflections and refractions in the line used by traveling wave relays during a fault event.

This paper aims twofold, first, to analyze the impact of TCSC controllers on transmission line conventional protection. Second, to propose an algorithm based on traveling waves and the Discrete Wavelet Transform (DWT), which must be capable of identifying the faulted line section and accurately calculating the distance to the fault (9), avoiding the TCSC effects.

1.1. TCSC Impact on Conventional Distance Protection

Let us consider a long transmission line compensated by a TCSC located in the middle of the line, as shown in Figure 1. During normal operating conditions, the TCSC is a variable capacitor in series with the transmission line. In this scheme, the TCSC impedance, Z_{TCSC}, compensates for some percentage of the series line impedance, Z_{LINE}. Therefore, the impedance measured by relay R_{A1} in the local end during normal operating conditions is

$$Z_{LINE\_COMP} = Z_{LINE} - Z_{TCSC} + Z_{LOAD}.$$

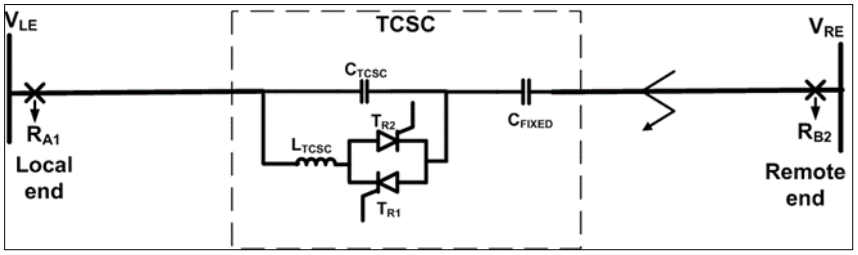

Figure 1 Transmission line and TCSC controller

However, during fault conditions, the situation is quite different, and two scenarios arise. These scenarios are fault events before and after the TCSC. In both cases, the magnitudes and behavior of the impedance measured by relay R_{A1} in Figure 1 are different.

A fault event before the TCSC does not represent a severe problem for the local relay R_{A1} since the fault impedance seen by the relay is given by $Z_{RA1} = Z_{LINE}$, which means that the impedance measured by the relay depends only on the line impedance up to the faulted point. Conventional distance relays are designed to deal with this scenario and operate reliably.

However, a fault event after the TCSC poses additional difficulties. In this case, the fault impedance seen by relay R_{A1} depends on the interaction between the TCSC and the transmission line. The impedance seen by relay R_{A1} is $Z_{RA1} = Z_{LINE} - Z_{TCSC}$. Therefore, the equivalent impedance due to the parallel connection of the TCSC inductance and capacitance must be accounted. From Figure 1, for a given compensation level, the TCSC equivalent impedance is (21):

$$X_{TCSC}(\alpha) = \frac{X_{CTCSC} X_{LTCSC}(\alpha)}{X_{LTCSC}(\alpha) - X_{CTCSC}} \quad \text{.....(1)}$$

Where:

$$X_{LTCSC}(\alpha) = X_{LTCSC} \frac{\pi}{\pi - 2\alpha - \sin 2\alpha}$$

$X_{LTCSC} = \omega L_{TCSC}$

$X_{CTCSC} = 1/(\omega C_{TCSC})$

α = Thyristors firing angle
$X_{FIXED} = 1/(\omega C_{FIXED})$

Figure 2 shows the behavior of the fault impedance seen by relay R_{A1} for a three-phase fault simulated along the transmission line shown in Figure 1 and several thyristor firing angles. For faults before the TCSC, the impedance seen by relay R_{A1} is a linear relationship where the impedance is proportional to the distance, as expected. At the TCSC location, a discontinuity is introduced by the FACTS device in the impedance-distance plane. The impedance drop depends on the line compensation level provided by the TCSC and can be negative. In this way, the faulted circuit is predominantly capacitive. Finally, the impedance increases linearly again, but this trend is shifted and slightly dependent on the thyristors firing angles. Table 1 shows the electrical parameters used for the electrical system depicted in Figure 1. Similar behavior is obtained for the impedance seen by R_{A1} for a single line to ground fault simulated along the line.

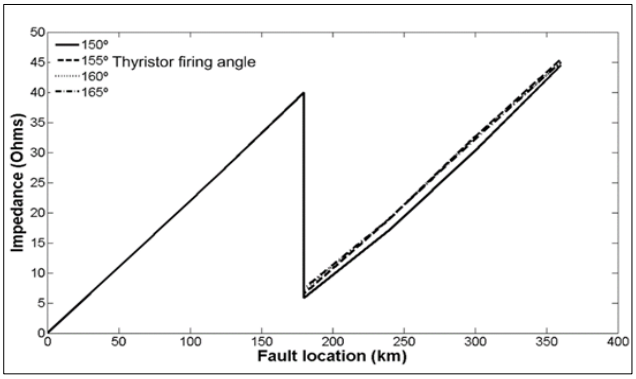

Figure 2 Impedance seen by R_{A1} for three phase faults along the line angles

Table 1 Electrical parameters

Parameter	Value
Line voltage	400 kV
Line length	360 km
Frequency	60 Hz
CTCSC	95 µF
CFIXED	98 µF
LTCSC	mH
Z0	550Ω

From Figure 2, it is evident that the behavior of the fault impedance may lead to relay over-reach for faults after the TCSC. Figure 3 shows on the X-R plane the above results where the Mho relay is set to protect some percentage of the transmission line length. The TCSC effect in the X-R plane is a steep drop in the impedance seen by the relay. Therefore, due to TCSC compensation, a fault after the controller seems closer to the relay. The error percentage in calculating the fault impedance depends on the TCSC compensation level at the moment of fault inception. Therefore, the reach and directionality of conventional distance protection relays are modified when the transmission line is compensated by a TCSC (22).

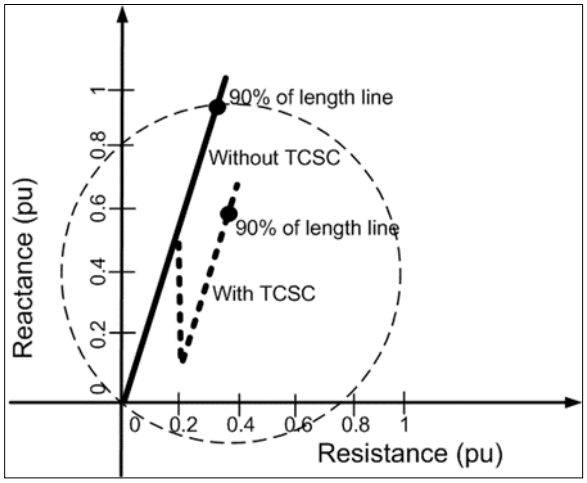

Figure 3 Over-reach caused by the TCSC controller

In addition, the TCSC effects in protective relaying are not limited to its line. The TCSC can also significantly affect distance relays on adjacent lines. To demonstrate this case, let us consider Figure 4, which shows the cascade connection of three transmission lines, one of them compensated with a TCSC.

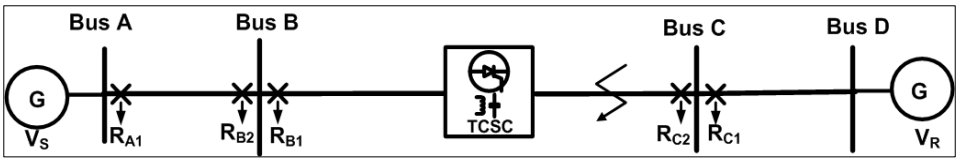

Figure 4 Cascade connection of transmission lines

In this case, the change on relay reach for R_{B1} due to the TCSC compensation is given by (4) (22):

$$\frac{Z_{LINE\_m}}{Z_{LINE\_m'}} = 1 + \frac{K}{m} \quad \text{.....(4)}$$

Where;
Z_{LINE_m}.- $mZ_{LINE}+Z_{TCSC}$
Z_{LINE_m}.-Line impedance measured at R_{B1}
Z_{LINE} .- Transmission line impedance
Z_{TCSC}.- TCSC impedance
m .- Fault location in per unit of line length
$Z_{LINE\_m'}$= mZ_{LINE} Measured impedance when for a fault at m.
K.- Compensation level Z_{TCSC}/Z_{LINE}

To assess the impact of TCSC compensation on adjacent lines, let us consider a three-phase fault at bus C and a TCSC compensation level of 70% (K=0.7). Let $Z_{AB} = Z_{BC} = Z_{CD}$. For relay R_{B1}, m=1, and $Z_{LINE\_m} = 0.3\ Z_{LINE}$. Under these conditions, R_{A1} and R_{B1} over-reach the fault, while relay R_{B2} has reverse over-reach for the same fault. Due to these inaccuracies R_{A1}, R_{B1} and R_{B2} are poorly coordinated to deal with the fault event.

In addition to over-reach, distance relays are prone to in-feed and out-feed conditions in highly interconnected power systems. From the above, new approaches and techniques are needed for fast fault detection and location in TCSC series compensated transmission lines.

2. Traveling Wave Approach for TCSC Compensated Transmission Lines.

2.1. Travelling Wave Approach

Traveling waves are electromagnetic pulses that provide helpful information to detect, locate and classify faults on transmission lines. They are generated during fault events when the line voltage collapses at the faulted point, producing abrupt changes in current. These sudden changes are the source of traveling waves propagating along the transmission line until they arrive at both lines' ends. Since at the end of the line typically there exist changes on the impedance seen by traveling waves, they are reflected back to the fault, where again they are refracted and reflected, and so on. Lattice diagrams have been traditionally used to illustrate this process. The outcome is a complex pattern of reflections and refractions, measured on each terminal by the local relay.

The above description is valid for transmission lines with no TCSC. However, when the device is connected to the line, the high-frequency traveling wave pattern of reflections and refractions is the same. This is because the TCSC behaves like a high pass filter at the frequencies associated with traveling wave pulses. Thus, when the TCSC thyristors are in open state conditions, the transmission line is connected in series with the TCSC capacitor C_{TCSC} and the capacitance C_{FIXED}, see Figure 1. Therefore, the equivalent capacitance at high frequencies represents a low-impedance path for traveling wave pulses.

On the other hand, when the TCSC thyristors are in a closed state, the transmission line is connected with C_{FIXED} and a parallel LC circuit, see Figure 1. Under this scenario, traveling wave pulses get through the TCSC capacitance because it represents a low-impedance path. There exists, however a resonant frequency due to the parallel LC circuit. This resonance condition occurs at relatively low frequencies; for example, for the values shown in Table 1, the resonant frequency is around a few hundred hertz. Therefore, for practical purposes, the risk of pulse distortion or attenuation is minimal. To support the above ideas, Figure 5 shows a fault event applied at t = 0.3 s in a transmission line with and without TCSC. Observe that, after filtering the low-frequency components, the high-frequency pattern of reflections and refractions in the line is the same; there is no distortion at the high frequencies generated during the fault event. On the other hand, Figure 6 shows the impedance seen by traveling wave pulses when they reach the TCSC terminals. Observe that after a few kHz, the traveling wave pulses get through the TCSC practically undisturbed. Since the TCSC has almost no effect on the traveling wave pattern, these high-frequency pulses can be used to detect and locate faults on the transmission line.

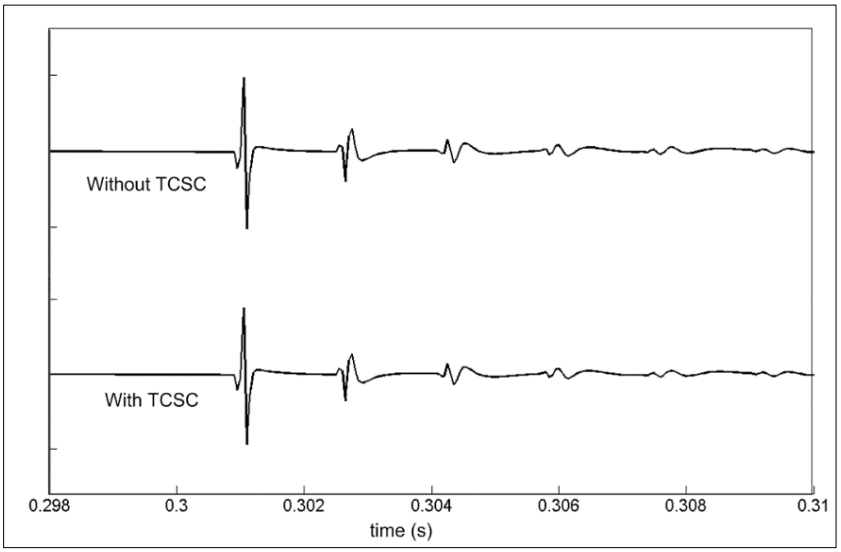

Figure 5 Traveling wave pattern during a fault with and without TCSC

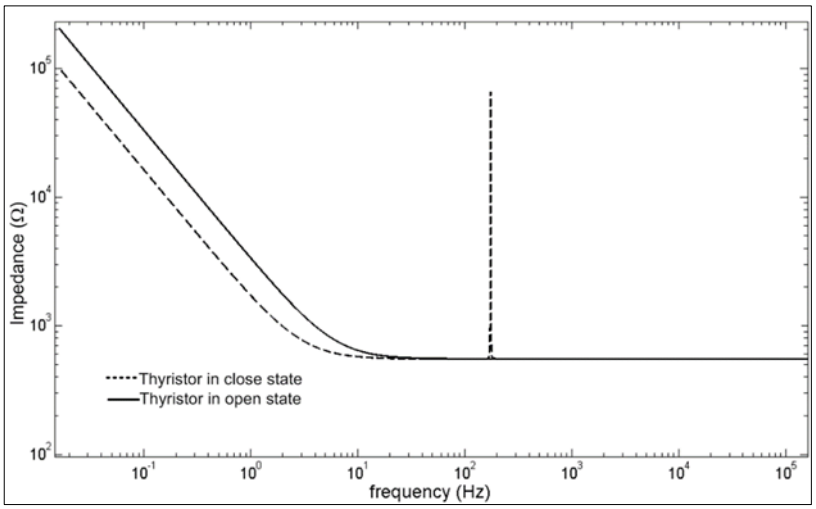

Figure 6 Impedance seen by travelling waves on arrival to TCSC terminals

2.2. Travelling waves and harmonic generated frequencies

It is well known that during operation the TCSC generates harmonic frequencies, mainly the third, fifth and seventh harmonic. These harmonic frequencies together with travelling waves are superimposed to the 60 Hz signal. For the development of the proposed algorithm it is desirable to separate travelling waves from harmonic frequencies in order to avoid any interaction that may distort the pattern of travelling wave pulses.

In this sense, the Discrete Wavelet Transform (DWT) is a powerful tool for analyzing transient events given its capability for discriminating high from low frequencies (23). This DWT characteristic facilitates the development of algorithms for high-speed protective relaying. The protection algorithm developed in this research uses the DWT applied to voltage and currents signals measured by the local relays. Both signals are filtered in stages and the detail coefficients (cD_Y) are obtained for different partition levels and bandwidths.

To separate high from low frequencies components, the DWT carry out two separated processing sequences aimed to obtain the approximation coefficients (cA_X) and detail coefficients (cD_Y). Both coefficients for the first partition level and voltage V_{LE} are calculated using (5) (24):

$$\begin{aligned} cA_1(t) &= \sum_k V_{LE}(t) L_d(k-2t) \\ cD_1(t) &= \sum_k V_{LE}(t) H_d(k-2t) \end{aligned} \quad \text{.....(5)}$$

Where; cA_1 is the approximation coefficient for level 1, cD_1 is the detail coefficient for level 1, L_d is a low-pass filter and H_d is the high-pass filter. Once the first set of coefficients is obtained, the above procedure is repeated several times until the desired level of partition for both coefficients is reached. This is represented by (6):

$$\begin{aligned} cA_{n+1}(t) &= \sum_k cA_n L_d(k-2t) \\ cD_{n+1}(t) &= \sum_k cA_n H_d(k-2t) \end{aligned} \quad \text{.....(6)}$$

where n is the number of partitions and $n \neq 1$. For a full description about the DWT process see (24).

An important aspect for the proposed algorithm is the fact that the bandwidth associated to each detail coefficient cD_Y depends on the sampling frequency. Table 2 shows the bandwidth for each cD_Y for a sampling frequency of 50 kHz. Consequently, in order to avoid any harmonic interaction between the TCSC generated frequencies and travelling waves due to the fault, the detail coefficients used by the algorithm must avoid any frequency close to the TCSC generated frequencies. From Table 2, the most suitable detail coefficient for this sampling frequency is level 1 because of its high bandwidth, far away from the harmonic frequencies generated by the TCSC.

Table 2 Bandwidth associated to cDY

Level of Detail Coefficient	Bandwidth
cD1 (level 1)	12.5 kHz to 25 kHz
cD2 (level 2)	6.25 kHz to 12.5 kHz
cD3 (level 3)	3.125 kHz to 6.25 kHz
cD4 (level 4)	1.562 Hz to 3.125 kHz
cD5 (level 5)	781.25 Hz to 1.562 kHz
cD6 (level 6)	390.6 Hz to 781.25 Hz
cD7 (level 7)	195.3 Hz to 390.6 Hz
cD8 (level 8)	97.6 Hz to 195.3 Hz

To verify the impact of TCSC generated harmonics in the detail coefficients cD_Y, Figure 7 show cD_1 and cD_7 calculated during a three-phase fault at 300 km from R_{A1} with and without TCSC. The fault was applied at t =0.3 s. Observe that cD_7 has some harmonic content when the TCSC is connected to the line. On the other hand, cD_1 has practically the same behavior with and without the TCSC, which means that cD_1 is not affected by the low harmonic frequencies generated by the TCSC. Consequently, the TCSC has no impact in the pattern of reflections and refractions in the line and this high frequency signal can be used for the development of protection algorithms for fault detection and location. Another feature is that cD_1 is better defined that cD_7 because of its higher bandwidth, according to Table 1. This characteristic facilitates fault location on the line.

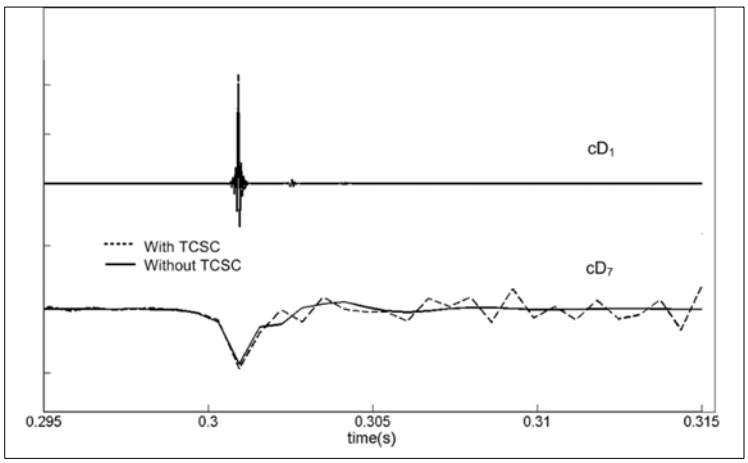

Figure 7 TCSC effects with different wavelet coefficients

As expected, the traveling wave is a good choice to avoid de TCSC effects on location algorithms.

2.3. Algorithm for fault detection and location

Figure 8 shows the main steps in the proposed algorithm to detect and locate faults in transmission lines with a TCSC controller. They are:

2.3.1. Obtain cD1 from VLE

V_{LE} is a vector of measured voltages in the local end by relay R_{A1}, see Figure 1, where V_{LE} is a vector with a window of five samples for each phase, V_A, V_B and V_C. V_{LE} is then transformed into the modal domain in order to eliminate mutual coupling between phases. The modal transformation is carried out using Clarke's transformation:

$$V_{LEM} = \begin{bmatrix} V_0 \\ V_1 \\ V_2 \end{bmatrix} = \begin{bmatrix} \frac{1}{\sqrt{3}} & \frac{1}{\sqrt{3}} & \frac{1}{\sqrt{3}} \\ \frac{\sqrt{2}}{\sqrt{3}} & \frac{-1}{\sqrt{6}} & \frac{-1}{\sqrt{6}} \\ 0 & \frac{1}{\sqrt{2}} & \frac{-1}{\sqrt{2}} \end{bmatrix} \begin{bmatrix} V_A \\ V_B \\ V_C \end{bmatrix}$$

Once the modal voltage V_{LEM} is obtained, cD_1 is calculated using (5). The coefficient cD_1 obtained is a vector containing the two aerial modes and the ground mode. Only the aerial mode 1 is used for detecting faults. The ground mode and the aerial mode 1 are used for locating faults. The same process is applied to the current signals in order to obtain its cD_1, which will be employed in step 2.

2.3.2. Fault detection

The DWT is applied to V_{LEM} and the coefficient cD_1 for the aerial mode 1 is obtained. The cD_1 magnitude is compared with a threshold value (cD_{1TH}) in order to detect a fault event in the transmission line. If cD_1 is greater than cD_{1TH} then a fault condition has been detected in the line. Another important task at this stage is a directional discrimination between a fault in the forward and backwards direction. The directional discrimination is accomplished by means of a polarity comparison between the coefficients of detail of both, voltage and current signals. This is explained in detail in section 4.3.

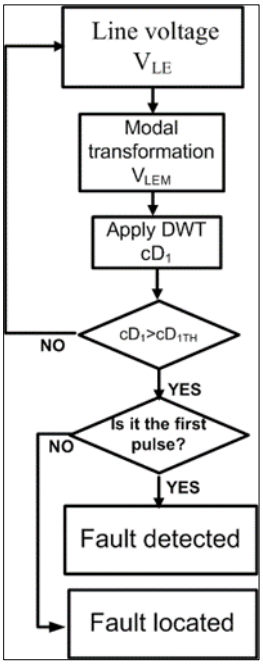

Figure 8 Flow chart to detect and locate faults

2.3.3. Fault location

The distance to the fault is calculated using the differences on time between the arrival of the first pulse to the local end at t_1 and the second pulse at t_2. In both cases the algorithm verifies that cD_1 is higher than cD_{1TH}. When t_1 and t_2 are obtained, the distance to the fault is calculated by (8) or (9) after proper discrimination (25)

$$FL = \frac{k_v(t_2 - t_1)}{2} \quad \text{.....(8)}$$

$$FL = T_{LL} - \frac{k_V(t_2 - t_1)}{2} \quad \text{.....(9)}$$

where k_v = 3x10^5 km/s is the speed of light, FL is the distance to the fault, T_{LL} is the transmission line length t_1 and t_2 are the arrival times for the first and second pulse to the local end. The time elapsed between t_1 and t_2 is proportional to the

distance from R_{A1} to the fault; this linear behavior will be verified in section 4.1. The choice between (8) and (9) is made considering the time elapsed between the first pulses of aerial mode 1 and the ground mode.

3. Results and discussion

The algorithm proposed was implemented in a PSCAD© and MATLAB© environment. In PSCAD© the electric circuit is solved and the input variables to the algorithm are generated, namely V_{LE} and I_{LE}. In MATLAB© the proposed algorithm processes all the received information and determines whether a fault condition exist in the line and where. It should be mentioned that this is a continuous process emulating an on-line simulation. After current and voltage signals are analyzed, the decision is sent to the travelling wave relay in order to trip the line or not. Figure 4 shows the proposed grid to assess the performance of FACTS devices on power systems. The TCSC and the transmission line selected for testing the proposed algorithm are located between bus B and C.

3.1. Relationship between fault distance and pulse arrival

Let us consider relay R_{B1} in Figure 4. In order to locate faults, the proposed algorithm requires a variable proportional to the fault distance, like the impedance measured by conventional distance relays. In addition, this variable must not be affected by the TCSC location and the compensation level in the line. Figure 9 shows the behavior of the variable $|t_2 - t_1|$ which is used in this study for fault location. Observe that the calculated distance to the fault is proportional to $|t_2 - t_1|$ and this relationship is linear and not affected whether the TCSC is connected to the line or not. Therefore, this variable is used in the proposed algorithm for fault location purposes on transmission lines. Several studies were carried out in order to verify that $|t_2 - t_1|$ is not dependent on the thyristors firing angle and line compensation level.

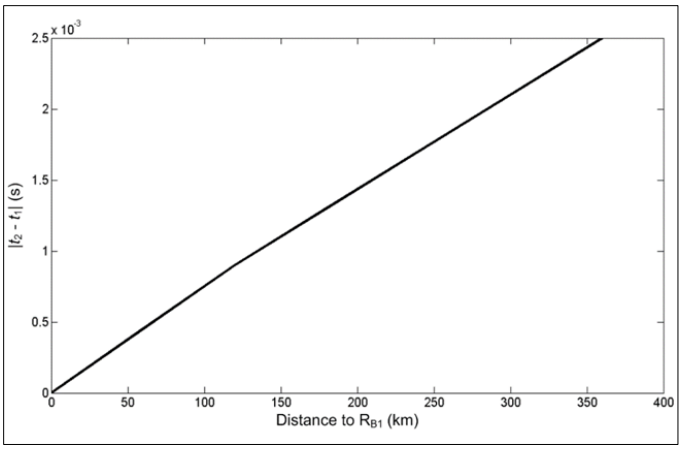

Figure 9 Linear relationship between $|t_2 - t_1|$ and the distance to the fault

3.2. Algorithm accuracy for locating faults

Table 3 Algorithm accuracy for fault location. Sampling rate 50 kHz

	Fault Type									
Fault location	**A-G**	**B-G**	**C-G**	**AB-G**	**AC-G**	**BC-G**	**ABC-G**	**AB**	**AC**	**BC**
30	29.98	29.98	29.98	29.98	29.98	29.98	29.98	29.98	29.98	29.98
120	122.91	122.91	122.91	122.91	122.91	119.92	119.92	119.92	122.91	119.92
180	182.87	179.87	182.87	182.87	182.87	182.87	182.87	182.87	182.87	182.87
240	239.83	239.83	239.83	239.83	242.83	242.83	242.83	242.83	242.83	242.83
300	296.79	299.79	296.79	296.79	299.79	299.79	299.79	299.79	299.79	299.79
360	362.75	362.75	362.75	362.75	362.75	362.75	362.75	362.75	362.75	362.75
Higher Error (%)	0.89	0.81	0.89	0.89	0.81	0.80	0.80	0.80	0.81	0.80

The algorithm performance for locating faults along its protection zone was evaluated. The algorithm was tested for balanced and unbalanced faults. Table 3 shows the real and calculated distance to the fault using the proposed algorithm described in this work. The maximum error in Table 3 is a percentage of the total line length.

Table 3 shows that in a TCSC environment, the algorithm can locate all type of faults with good accuracy. For a sampling frequency of 50 kHz, the error in calculating the distance to the fault is smaller than 1%. This error is mainly due to the sampling frequency used, 50 kHz, which provides a resolution of 3.2 km between samples. The algorithm was tested using different fault conditions like different fault resistances, variable power factor and thyristor firing angles and line compensation level. In all the cases, the algorithm was capable of detecting and locating the fault with good accuracy, smaller than 1% of the total line length.

The impact of fault inception angle was also analyzed. The study consisted in applying faults with inception angles close to zero crossing, the more critical case. The results show the algorithm has an error for calculating the fault distance < 1% as long as the voltages is greater than 3% of nominal voltage. For smaller voltages the approach proposed in (26), based on current measurements and the ground mode, can be incorporated easily to the model in order to increase its application range.

3.3. Protection of adjacent non-compensated lines.

In power networks it is important to discriminate faults in the forward direction from faults in the backwards direction. The proposed algorithm fulfills this basic requirement by using current and voltage pulses polarities. Figure 10 shows in detail the current and voltage pulses calculate by relay R_{B1} for a fault located at 50% of line BC, see Figure 4. Relay R_{B1} determines that the fault is in the forward direction because voltage and current pulses polarities are opposite, tripping the line. On the other hand, R_{B2} determines that the fault is in the backward direction because current and voltage pulses polarities are the same. Since the fault was detected behind the relay, R_{B2} does not trip line BC

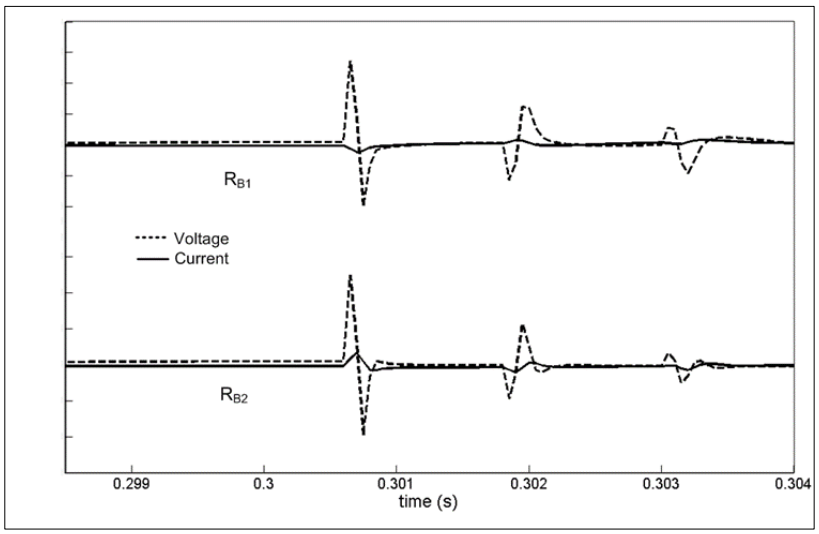

Figure 10 Traveling wave pulses calculated by R_{B1} and R_{B2}

Relay reach is another important topic for transmission line protection. Figure 11 show voltage and current pulses during a three-phase fault at 90% of line BC. In this particular case, the difference on pulse arrival $|t_2 - t_1|$ = 2.16 ms determines the reach of R_{B1} and its first operating zone. Therefore, if $|t_2 - t_1| > 2.16$ ms, the fault is located in R_{B1} second zone of protection, whose extension depends on the length of line CD. For illustrative purposes, a second fault is simulated at 50% of line CD. The pattern of pulses seen by R_{B1} is also shown on Figure 11. Observe that pulse separation is greater than 2.16 ms which means that the fault is located in R_{B1} second zone of operation. In brief, pulse polarities determine fault direction (forward and backward) and pulse separation determines distance to the fault and the corresponding relay operation zone.

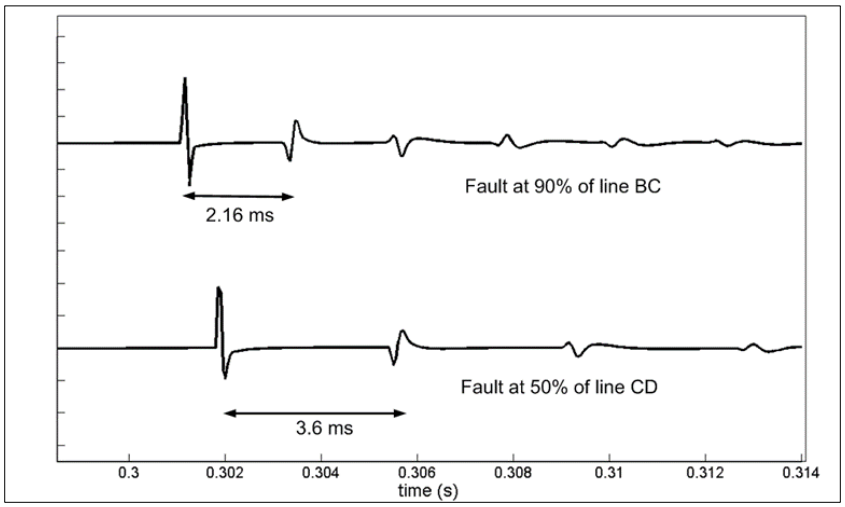

Figure 11 Traveling waves seen by R_{B1}

For the system shown in Figure 4, Table 4 shows different faults simulated at different locations and the operation zone on which the different relays classify the fault. Unlike the results shown in (22), the proposed algorithm determines in a proper way the right operation zone for faults on adjacent lines.

Table 4 Protection Zone by relays under different positions of faults

Fault position	**R_{A1}**	**R_{B2}**	**R_{B1}**	**R_{C1}**
50-90% of line AB	Zone I	Zone I		
90-100% of line AB	Zone II	Zone I		
0-50% of line BC	Zone II		Zone I	
50-90% of line BC	Zone III		Zone I	
90-100% of line BC			Zone II	
0-50% of line CD			Zone II	Zone I

4. Conclusion

The inclusion of TCSC controllers on transmission lines produce undesirable effects in the impedance seen by conventional distance relays, which may lead to relay over-reach and undesirable tripping. In order to overcome these difficulties associated to the application of FACTS devices on electrical networks the use of traveling waves is a good option.

The DWT is an alternative to analyze transient events like faults on transmission lines because of its undoubted capability to discriminate high from low frequency components. The analysis and computer simulations carried out in this paper show that the TCSC behaves like a high pass filter, independently of the thyristor firing angles. Therefore, by selecting a suitable sampling frequency and detail coefficients in the DWT, it is possible to avoid the effect of harmonic frequencies generated by the TCSC during the signal processing. In this way, the pattern of travelling waves generated during the fault event can be used undistorted by relays algorithms for detecting and locating faults on transmission lines with TCSC controllers.

A relay algorithm for detecting faults on transmission lines with TCSC controllers has been presented in this paper. The proposed algorithm is based in modal analysis and the DWT. The developed methodology analyzes the high frequency voltage and current pulses as well as its delays and polarities in order to detect and locate faults on transmission lines. The algorithm was developed in a PSCAD-MATLAB environment and works emulating an on-line relay process.

Several studies were carried out in order to verify the algorithm accuracy. The first study is aimed to obtain a variable proportional to the fault distance, $|t_2 - t_1|$, which must be independent of the line compensation level and thyristor firing

angle, two important parameters during TCSC operation. The second study allowed determining the algorithm accuracy for detecting and locating faults. The results show that the error in calculating the distance to the fault is < 1% for a sampling rate of 50 kHz, which is considered acceptable for relaying purposes. For higher sampling rates the algorithm accuracy is improved. Studies were also carried out considering variable fault resistances, load angle and fault inception angles. The computer results show that algorithm accuracy remains practically unchanged, < 1% of the total line length.

Compliance with ethical standards

Acknowledgments

This work was supported by National Technological of Mexico under the grant 13878.22-P.

Disclosure of conflict of interest

The Authors confirm that the content of this manuscript has no conflict of interest.

References

[1] Fathollahi A, Kargar A, Yaser Derakhshandeh S. Enhancement of power system transient stability and voltage regulation performance with decentralized synergetic TCSC controller. Int J Electr Power Energy Syst. 2022 Feb 1 135: 107533.

[2] Lee HJ, Kim SH, Hur K, Choi JS, Oh HJ, Lee BJ, et al. Integrating TCSC to enhance transmission capability and security: Feasibility studies for Korean electric power system. IEEE Power Energy Soc Gen Meet. 2016 Nov 10 2016-November.

[3] Singh S, Pujan Jaiswal S. Enhancement of ATC of micro grid by optimal placement of TCSC. Mater Today Proc. 2021 Jan 1 34:787–92.

[4] Aslam W, Xu Y, Siddique A, Nawaz A, Rasheed M. Electrical Power System Stability Enhancement by Using an Optimal Fuzzy PID Controller for TCSC with Dual TCRs. 2018 IEEE 3rd Int Conf Integr Circuits Microsystems, ICICM 2018. 2018 Dec 28 231–4.

[5] Zare K, Hagh MT, Morsali J. Effective oscillation damping of an interconnected multi-source power system with automatic generation control and TCSC. Int J Electr Power Energy Syst. 2015 Feb 1 65:220–30.

[6] Ghorbani A, Mehrjerdi H, Heydari H, Ghanimati S. A pilot protection algorithm for TCSC compensated transmission line with accurate fault location capability. Int J Electr Power Energy Syst. 2020 Nov 1 122:106191.

[7] Shateri H, Kazemi A, Jamali S. Impacts of TCSC on Distance Relay Performance. Int Rev Electr Eng. 5(6).

[8] Dash PK, Samantray SR. Phase selection and fault section identification in thyristor controlled series compensated line using discrete wavelet transform. Int J Electr Power Energy Syst. 2004 Nov 1 26(9):725–32.

[9] Dash PK, Samantaray SR, Panda G. Fault classification and section identification of an advanced series-compensated transmission line using support vector machine. IEEE Trans Power Deliv. 2007 Jan 22(1):67–73.

[10] Ahsaee MG, Sadeh J. A novel fault-location algorithm for long transmission lines compensated by series FACTS devices. IEEE Trans Power Deliv. 2011 Oct 26(4):2299–308.

[11] Nobakhti SM, Akhbari M. A new algorithm for fault location in series compensated transmission lines with TCSC. Int J Electr Power Energy Syst. 2014 May 1 57:79–89.

[12] Mohamed AAR, Sharaf HM, Ibrahim DK. Enhancing Distance Protection of Long Transmission Lines Compensated with TCSC and Connected with Wind Power. IEEE Access. 2021 9:46717–30.

[13] Sahoo B, Samantaray SR. An enhanced fault detection and location estimation method for TCSC compensated line connecting wind farm. Int J Electr Power Energy Syst. 2018 Mar 1 96:432–41.

[14] Dasgupta A, Nath S, Das A. Transmission Line Fault Classification and Location Using Wavelet Entropy and Neural Network. http://dx.doi.org/101080/153250082012716495 [Internet]. 2012 Oct 1 [cited 2022 Dec 3] 40(15):1676–89. Available from: https://www.tandfonline.com/doi/abs/10.1080/15325008.2012.716495

[15] Wang D, Hou M, Guo Y. Travelling Wave Fault Location of HVAC Transmission Line Based on Frequency-Dependent Characteristic. IEEE Trans Power Deliv. 2021 Dec 1 36(6):3496–505.

[16] Liang R, Peng N, Zhou L, Meng X, Hu Y, Shen Y, et al. Fault Location Method in Power Network by Applying Accurate Information of Arrival Time Differences of Modal Traveling Waves. IEEE Trans Ind Informatics. 2020 May 1 16(5):3124–32.

[17] Zhang C, Song G, Wang T, Dong X. An Improved Non-Unit Traveling Wave Protection Method with Adaptive Threshold Value and Its Application in HVDC Grids. IEEE Trans Power Deliv. 2020 Aug 1 35(4):1800–11.

[18] Saleh KA, Hooshyar A, El-Saadany EF, Zeineldin HH. Protection of High-Voltage DC Grids Using Traveling-Wave Frequency Characteristics. IEEE Syst J. 2020 Sep 1 14(3):4284–95.

[19] Pei X, Pang H, Li Y, Chen L, DIng X, Tang G. A Novel Ultra-High-Speed Traveling-Wave Protection Principle for VSC-based DC Grids. IEEE Access. 2019 7:119765–73.

[20] Vázquez E, Castruita J, Chacon OL, Conde A. A new approach traveling-wave distance protection - Part I: Algorithm. IEEE Trans Power Deliv. 2007 Apr 22(2):795–800.

[21] Understanding FACTS: Concepts and Technology of Flexible AC Transmission Systems | IEEE eBooks | IEEE Xplore [Internet]. [cited 2022 Dec 3]. Available from: https://ieeexplore.ieee.org/book/5264253

[22] Khederzadeh M, Sidhu TS. Impact of TCSC on the protection of transmission lines. IEEE Trans Power Deliv. 2006 Jan 21(1):80–7.

[23] Beg MA, Khedkar MK, Paraskar SR, Dhole GM. Feed-forward Artificial Neural Network–Discrete Wavelet Transform Approach to Classify Power System Transients. http://dx.doi.org/101080/153250082012755235 [Internet]. 2013 Apr 1 [cited 2022 Dec 3] 41(6):586–604. Available from: https://www.tandfonline.com/doi/abs/10.1080/15325008.2012.755235

[24] Misiti M, Misiti Y, Oppenheim G, Poggi J-M. Wavelet ToolboxTM 4 User's Guide. 2009 [cited 2022 Dec 3] Available from: www.mathworks.com

[25] Magnago FH, Abur A. Fault location using wavelets. IEEE Trans Power Deliv. 1998 13(4):1475–80.

[26] García-Gracia M, Montañés A, El Halabi N, Comech MP. High resistive zero-crossing instant faults detection and location scheme based on wavelet analysis. Electr Power Syst Res. 2012 Nov 1 92:138–44.